J. of the Chosun Natural Science
Vol. 6, No. 3 (2013) pp. 183 – 186
http://dx.doi.org/10.13160/ricns.2013.6.3.183

Well Defined One-Dimensional Photonic Crystal Templated by Rugate Porous Silicon

Sung Gi Lee†

Abstract

Well defined 1-dimentional (1-D) photonic crystals of polystyrene replicas have been successfully obtained by removing the porous silicon from the free-standing rugate porous silicon/phenylmethylpolysiloxane composite film. Rugate porous silicon was prepared by an electrochemical etching of silicon wafer in HF/ethanol mixture solution. Exfoliated rugate porous silicon was obtained by an electropolishing condition. A composite of rugate porous silicon/ phenylmethylpolysiloxane composite film was prepared by casting a toluene solution of phenylmethylpolysiloxane onto the top of rugate porous silicon film. After the removal of the template by chemical dissolution, the phenylmethylpolysiloxane castings replicate the photonic features and the nanostructure of the master. The photonic phenylmethylpolysiloxane replicas are robust and flexible in ambient condition and exhibit an excellent reflectivity in their reflective spectra. The photonic band gaps of replicas are narrower than that of typical semiconductor quantum dots.

Key words: Porous Silicon, phenylmethylpolysiloxane, Template, Rugate Structure

1. Introduction

Preparation of complex nano-structure materials is one of the greatest interest as a useful and versatile technique to provide the use of photonic crystals for chemical and biological sensors, high throughput screening, and controlled release of drug delivery[1-12]. Rugate porous silicon[13] is an attractive candidate for building nano-structure composite materials because the porosity and average pore size can be tuned by adjusting an electrochemical preparation conditions which allow the construction of photonic crystals[14-19]. Rugate porous silicon exhibits unique optical properties such as an excellent reflectivity with a narrow full width at half maximum in specific wavelength. The rugate porous silicon films can be easily lifted off from the silicon substrate to obtain a free-standing rugate porous silicon films. For many applications, free-standing rugate porous silicon is limited due to its chemical and mechanical stability. These free-standing films are easily air-oxidized and very brittle. The flexible rugate porous silicon/phenylmethylpolysiloxane composite materials eliminate these issues and improve chemical and mechanical stability. However, these composite materials are not suitable for the application of biological sensors *in vivo* due to the presence of silicon metal of the porous silicon films. Therefore, biocompatible phenylmethylpolysiloxanes such as a phenylmethylpolysiloxane showing a specific optical properties would be ideal for these applications. Here, we have prepared photonic crystals of phenylmethylpolysiloxane showing a high reflectivity. Casting of phenylmethylpolysiloxane solution onto a porous silicon dioxide layer and dissolving of porous silicon layer provides the means for the construction of complex photonic structures with phenylmethylpolysiloxanes.

2. Experimental Section

Rugate porous silicon containing nanometer-scale pores is prepared by an anodic electrochemical etch of p++-type silicon wafer whose resistivity is between 0.8-0.2 mΩ·cm. The etching solution consisted of a 3:1 volume mixture of aqueous 48% hydrofluoric acid (ACS reagent, Aldrich Chemicals) and absolute ethanol (ACS reagent, Aldrich Chemicals). Galvanostatic etching has been carried out in a Teflon cell using a two-electrode

Korea Institute of Science and Technology, P.O. Box 131, Cheongryang, seoul 130-650, Korea

†Corresponding author : sg_lee0808@naver.com
(Received : August 27, 2013, Revised : September 16, 2013, Accepted : September 23, 2013)

configuration. The applied current density is modulated with a pseudo sine wave (typically between 11.5 mA/cm^2 and 34.6 mA/cm^2, 18 s periodicity, 100 repeats) to generate a periodically varying porosity gradient. The resulting rugate porous silicon film has been removed from the substrate by applying an lift-off current at 480 mA/cm^2 for 2 min and 30 mA/cm^2 for 2 min. Then the free-standing rugate porous silicon films are thermally oxidized in the furnace at 450°C for 3 h. In a typical preparation, 4 g of phenylmethylpolysiloxane (Aldrich, M_w = 280,000) are dissolved in 20 mL of toluene (Fisher Scientific). The toluene solution has been cast on the top surface of free-standing porous silicon film. The resulting composite films have been annealed at 95°C for 20 min. Then porous silicon has been removed in aqueous 8% HF solution. After the removal of the template by chemical dissolution, the phenylmethylpolysiloxane castings replicate the photonic features and the nanostructure of the master. Optical reflectivity spectra are measured using a tungsten-halogen lamp and an Ocean Optics S2000 CCD spectrometer fitted with a fiber optic input. The reflected light collection end of the fiber optic is positioned at the focal plane of the optical microscope.

3. Results and Discussion

Multilayered porous silicon containing rugate porosities has been successfully prepared by using a periodic galvanostatic electrochemical etch of crystalline silicon. Free-standing rugate porous silicon films have been obtained from the silicon substrate by an applying of lift-up current in a solution of HF and ethanol. The thermal oxidation of free-standing rugate porous silicon film results the reflectivity shifted to shorter wavelengths. This rugate porous silicon dioxide films are typically very brittle and shatter when subjected to minor shear stresses. FE-SEM image of rugate porous silicon template is shown in Fig. 1. FE-SEM image of rugate porous silicon as shown in Fig. 1 indicated that the prepared rugate porous silicon had cylindrical mesopores with an even pore size.

After the thermal oxidation of rugate porous silicon films, the presence of silicon oxide has been determined by FT-IR measurement. The FT-IR spectra of the oxidized rugate porous silicon shown in Fig. 2 display absorption bands characteristic of silicon oxide. The FT-

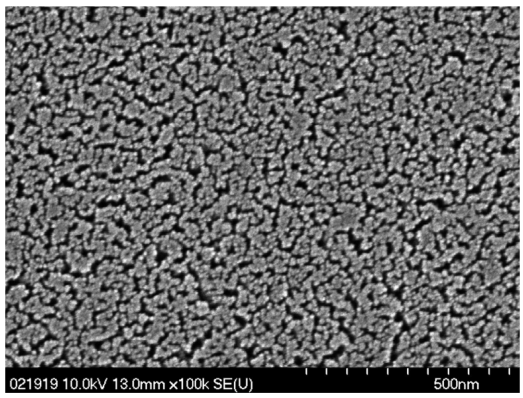

Fig. 1. FE-SEM image of free-standing rugate porous silicon film.

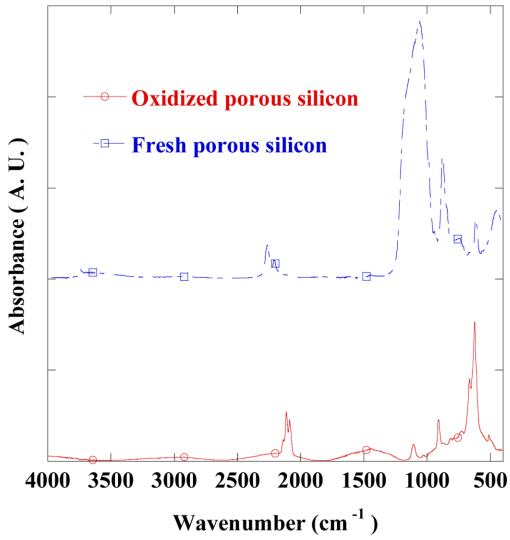

Fig. 2. FT-IR spectra of free-standing rugate porous silicon film and oxidized rugate porous silicon film.

IR spectrum of a fresh rugate porous silicon film displayed vibrational bands in the fingerprint region of the spectrum. υ(Si-H) and δ(Si-H) vibrations associated with surface Si-H species were also apparent at 2117 and 941 cm^{-1}, respectively. The oxidized rugate porous silicon film exhibited vibrational bands characteristic of the υ(OSi-H), δ(OSi-H), and υ(Si-O) vibrational modes were observed at 2270, 881, and 1070 cm^{-1}, respectively.

Dissolved phenylmethylpolysiloxane in toluene solution has been cast on the top surface of oxidized rugate porous silicon films. The resulting composite films have been annealed to fill the pore with phenylmethylpolysi-

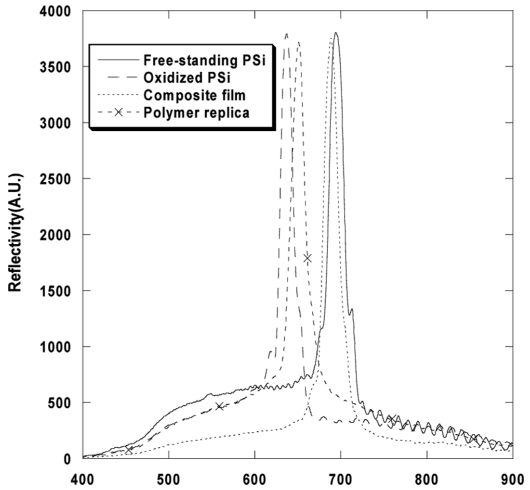

Fig. 3. Reflection spectra of oxidized rugate porous silicon, phenylmethylpolysiloxane replica, rugate porous silicon/phenylmethylpolysiloxane composite film, and free-standing rugate porous silicon film (from left).

loxane completely. The spectral feature of oxidized rugate porous silicon/phenylmethylpolysiloxane composite film from optical interference is shifted to longer wavelengths upon introduction of the polymer into the pores of rugate porous silicon.

The oxidized rugate porous silicon template has been removed from the composite films in aqueous 8% HF solution. After the removal of the oxidized rugate porous silicon template by chemical dissolution, the polymer castings replicate the photonic features and the nanostructure of the master. The polymer replica exhibits its reflection shifted to shorter wavelengths. This blue shift indicates that the removal of oxidized rugate porous silicon template by chemical dissolution results the decrease of refractive index.

The photonic crystals of rugate porous silicon display a very sharp line in the optical reflectivity spectrum shown in Fig. 3. Prepared rugate porous silicon exhibits a high reflectivity at 700 nm. The spectral band of rugate porous silicon has a full-width at half-maximum of 20 nm. The reflection resonance of free-standing rugate porous silicon film also displayed reflection peak at the identical location. The thermal oxidation of free-standing rugate porous silicon film results the reflectivity at 640 nm shifted to shorter wavelengths, due to the decrease of refractive index of silicon dioxide from silicon. The spectral feature of rugate porous silicon/phenylmethylpolysiloxane composite film from optical interference appears at 690 nm which shifted to longer wavelengths by the introduction of the phenylmethylpolysiloxane. Such a large red shift is characteristic of an increase in the average refractive index of the porous silicon layers, consistent with the replacement of a significant amount of empty pore volume with phenylmethylpolysiloxane. After removal of porous silicon from the composite film, the phenylmethylpolysiloxane replica exhibits its reflection at 650 nm shifted to shorter wavelengths.

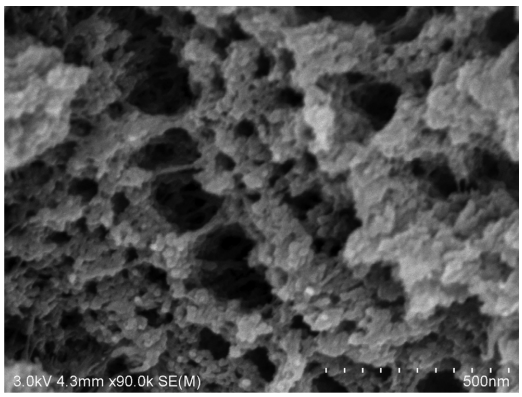

Fig. 4. FE-SEM image of photonic crystal of phenylmethylpolysiloxane.

FE-SEM image of photonic crystal of phenylmethylpolysiloxane is shown in Fig. 4. FE-SEM image of photonic crystal of phenylmethylpolysiloxane indicated that photonic crystal of phenylmethylpolysiloxane had cylindrical macropores. The photonic band gaps of replicas are about 14 nm which is narrower than that of typical semiconductor quantum dots. These phenylmethylpolysiloxane replicas could be useful for a possible applications.

4. Conclusions

The photonic phenylmethylpolysiloxane replicas showing a desired reflectivity by casting of phenylmethylpolysiloxane solution onto a porous silicon dioxide multilayer have been prepared. The photonic phenylmethylpolysiloxane replicas are robust in ambient condition and exhibit an excellent reflectivity in their reflective spectra. The photonic band gaps of replicas are narrower than that of typical semiconductor quantum dots. The means for the construction of complex

photonic structures with phenylmethylpolysiloxanes have been provided.

References

[1] H. Sohn, S. Letant, M. J. Sailor, and C. Trogler, "Detection of fluorophosphonate chemical warfare agents by catalytic hydrolysis with a porous silicon interferometer", J. Am. Chem. Soc. Vol. 122, pp. 5399-5400, 2000.

[2] M. W. Hwang and S. D. Cho, "Detection of organic vapors using change of Fabry-Perot fringe pattern of surface functionalized porous silicon", J. Chosun Natural Sci., Vol. 3, pp. 168-173, 2010.

[3] D. H. Jung, "Biosensor based on distributed Bragg reflector photonic crystals for the detection of protein A", J. Chosun Natural Sci., Vol. 3, pp. 33-37, 2010.

[4] S. D. Cho, "Preparation of polystyrene thin films containing Bragg structure and investigation of their photonic characteristics", J. Chosun Natural Sci., Vol. 3, pp. 138-142, 2010.

[5] S. D. Cho, "Detection of nitroaromatic compounds with functionalized porous silicon using quenching photoluminescence", J. Chosun Natural Sci., Vol. 3, pp. 202-205, 2010.

[6] Y. D. Koh, "Analysis on oxidation of porous silica obtained from thermal oxidation of porous silicon", J. Chosun Natural Sci., Vol. 3, pp. 153-156, 2010.

[7] J. M. Han, "Photoluminescence of porous silicon according to various etching times and various applied current densities", J. Chosun Natural Sci., Vol. 3, No. 3, pp. 148-152, 2010.

[8] S. H. Jang, "Study on thickness of porous silicon layer according to the various anodization times", J. Chosun Natural Sci., Vol. 3, pp. 206-209, 2010.

[9] K. S. Jung, "Fabrication and characterization of DBR porous silicon chip for the detection of chemical nerve agents", J. Chosun Natural Sci., Vol. 3, pp. 237-240, 2010.

[10] Y. C. Koh, "1-D photonic crystals based on Bragg structure for sensing and drug delivery applications", J. Chosun Natural Sci., Vol. 4, pp. 11-14, 2011.

[11] S. G. Kim, "Optical characterization of smart dust based on photonic crystals and its sensing applications", J. Chosun Natural Sci., Vol. 4, pp. 7-10, 2011.

[12] S. H. Jang, "Chemical and physical properties of porous silicon", J. Chosun Natural Sci., Vol. 4, pp. 1-6, 2011.

[13] Y. Y. Li, F. Cunin, J. R. Link, T. Gao, R. E. Betts, S. H, Reiver, V. Chin, S. N. Bhatia, M. J. Sailor, "Polymer replicas Photonic porous silicon for sensing and drug delivery applications", Science, 2003, *28*, 299.

[14] M. Qian, X. Q. Bao, L. W. Wang, X. Lu, J. Shao, X. S. Chen, "Structural tailoring of multilayer porous silicon for photonic crystal application", J. Cryst. Growth, 2006, 292, 347-350.

[15] B.-Y. Lee, M. Hwang, H. Cho, H.-C. Kim, and S. Jang, "Characterization and surface-derivatization of porous silicon", J. Chosun Natural Sci., Vol. 4, pp. 182-186, 2011.

[16] B.-Y. Lee, M. Hwang, H. Cho, H.-C. Kim, and S. Jang, "Chemical and physical properties of porous silicon", J. Chosun Natural Sci., Vol. 4, pp. 187-191, 2011.

[17] B.-Y. Lee, M. Hwang, H. Cho, H.-C. Kim, and S. Cho, "Multiple-bit encodings of bragg photonic-structures by using consecutive etch with various square wave currents", J. Chosun Natural Sci., Vol. 4, pp. 192-196, 2011.

[18] B. Kim, "Investigation of relationship between reflection resonance and applied current density in bragg photonic crystal", J. Chosun Natural Sci., Vol. 5, pp. 27-31, 2011.

[19] S. Jang, "Investigation of the changes of Fabry-Perot fringe patterns in porous silicon during etching process", J. Chosun Natural Sci., Vol. 5, pp. 13-17, 2011.